Evaluation of Gd-EOB-DTPA Uptake in a Perfused and Isolated Mouse Liver Model

Correlation Between Magnetic Resonance Imaging and Monochromatic Quantitative Computed Tomography

Jérôme Segers, PhD, Géraldine Le Duc, PhD,† Catherine Laumonier, PhD,* Irène Troprès, PhD,†‡ Luce Vander Elst, PhD,* and Robert N. Muller, PhD**

Objectives: The aim of this work was to quantitatively evaluate the pharmacokinetic pattern of Gd-EOB-DTPA in a model of isolated and perfused mouse liver by using magnetic resonance imaging (MRI) and monochromatic quantitative computed tomography (MQCT).

Materials and Methods: For MQCT, perfusions were realized with the gallbladder spared; for MRI, with gallbladder spared, severed, or clamped. Inductively coupled plasma (ICP) was performed at the end of the imaging protocols.

Results: MQCT, MRI, and ICP showed that perfused mice livers with spared gallbladder can be divided in 2 groups depending on their uptake profile of the contrast agent. Livers with severed gallbladders behave as the group internalizing more contrast agent, whereas Gd-EOB-DTPA uptake looks impaired in the case of a clamped gallbladder.

Conclusions: For the first time, MQCT and MRI have been performed in parallel to investigate the same physiological problem. The existence of 2 liver groups seems to be the result of some instability of the protocol likely to be related to surgery.

Key Words: monochromatic quantitative computed tomography, MRI, Gd-EOB-DTPA, mice perfused liver

(*Invest Radiol* 2005;40: 574–582)

Received November 24, 2004 and accepted for publication, after revision, April 14, 2005.

From the *Department of Organic and Biomedical Chemistry, NMR and Molecular Imaging Laboratory, University of Mons-Hainaut, Mons, Belgium; †Biomedical Beamline, European Synchrotron Radiation Facility, Grenoble, France; and the ‡3T MRI unit, CHU, Grenoble, France.

Reprints: Robert N. Muller, PhD, Department of Organic and Biomedical Chemistry, NMR and Molecular Imaging Laboratory, University of Mons-Hainaut Avenue du Champ de Mars, B-7000 Mons, Belgium. E-mail: robert.muller@umh.ac.be.

ISSN: 0020-9996/05/4009-0574

Gd-EOB-DTPA (Primovist, Schering AG, Berlin, Germany) is a paramagnetic complex designed as a hepatotropic magnetic resonance imaging (MRI) contrast agent (CA) excreted by the biliary route. Its synthesis and physicochemical characterization have been extensively described.[1–3] Gd-EOB-DTPA enters into the hepatocytes through the organic anion transporter (OATP) system located on the membrane, which is involved in the hepatocellular uptake of bilirubin. Once inside the hepatocytes, Gd-EOB-DTPA is transported through the cell in a nonmetabolized form to the bile canaliculi by the glutathione-S-transferase transporter.[4–6] Gd-EOB-DTPA has proved to be useful to evaluate liver functions and dysfunctions such as hepatitis, as well as to evidence both liver metastasis and hepatocellular carcinoma.[7–14] The possibility to detect tumors within the liver is increased because undifferentiated neoplastic cells, which lack anion-transport and phagocytic functions, cannot extract Gd-EOB-DTPA from the blood.[9,10] In the case of hepatitis, the level of liver enhancement is decreased and the washout phase is prolonged.[12]

Contrast-enhanced MRI is recognized as a powerful tool for the assessment of functional parameters. However, the quantitative interpretation of the CA effect on image intensity is not straightforward because the MR signal is a complex function of CA characteristics (eg, in situ relaxivities, magnetic susceptibility, concentration, biodistribution) as well as of experimental parameters (eg, magnetic field, echo time, repetition time).[5] MRI CAs contribute to both T_1 and T_2 relaxation processes and can thus induce opposite effects on the contrast. For these reasons, CA concentration is difficult to obtain from image intensity measurements. Therefore, quantitative evaluation of gadolinium-based systems is usually carried out by inductively coupled plasma atomic emission spectrometry (ICP-AES) or high-performance liquid chromatography (HPLC) at the expense of spatial resolution, real-time follow up, and a large number of animals. In

computed x-ray tomography (CT) as well as in micro-CT, the direct relationship between the Hounsfield units (HU) and the local concentration of the agent is a great advantage. Nevertheless, high accuracy measurements are not achievable as a result of the relatively low concentration of gadolinium and the broad energy spectrum of x-ray tubes that induce beam-hardening effects and also scattered radiation. In the particular case of micro-CT, a high spatial resolution is possible at the expense of temporal resolution. Among CT methods, an alternative technique called monochromatic quantitative computed tomography (MQCT)[15,16] has recently been implemented and highlighted as a complementary tool to other imaging techniques in the field of preclinical research.[17–20] As a result of the monochromaticity of the synchrotron beam, this technique allows for nondestructive, real-time, and absolute quantitative in vivo measurements of Gd concentration with a fair spatial resolution of 350 μm.[19,21]

The aim of this study was to evaluate the pharmacokinetic pattern of Gd-EOB-DTPA in a model of isolated and perfused mouse livers by both the MRI and MQCT techniques and to cross-correlate the results.

MATERIALS AND METHODS

Perfusion Protocol

Three protocols of liver perfusion were carried out: the gallbladder was spared, severed, or clamped. Severing and clamping were performed once the liver was perfused and isolated. The perfusion protocol was adapted to mice from a protocol previously established on rats.[22–26] Hepatic perfusion consists of the administration to the liver of a blood-substituting solution, maintained at body temperature in water-jacketed chambers and delivered through a thermostated umbilical line at constant flow, sufficient to provide correct nutrition and oxygenation to the tissue. The perfusion medium was a phosphate-free Krebs-Henseleit (KH) solution buffered with bicarbonate and containing (in mM) NaCl (118.0), KCl (4.7), $CaCl_2$ (3.0), $MgSO_4$ (1.2), Na_2EDTA (0.5), $NaHCO_3$ (25.0), and D-Glucose (5.5) (Sigma-Aldrich, Bornem, Belgium). The perfusion buffer was saturated by carbogene (O_2: 95%, CO_2: 5%), providing optimum oxygenation and ensuring a constant pH value at 7.40 by formation of a bicarbonate buffer system. The perfusion buffer solution entered the liver by the portal vein and was ejected by the severed sus-hepatic vein. A peristaltic pump (7521-10; Cole-Parmer Instruments, Chicago, IL) was used for this purpose supplied with 2 heads equipped with Masterflex tubes (Cole-Parmer Instruments). One head provides the perfusate to the liver at the chosen flow rate while the other recovers it at twice the flow rate.

Mice (males Balb/cByJIco, 5–6 weeks old, Charles River, L'Arbresle, France, for MQCT and B&K Universal Limited Hull, U.K., for MRI) were anesthetized by an intraperitoneal injection of 50 mg/kg sodium pentobarbital (Nembutal; CEVA, Brussels, Belgium). A median laparotomy was performed to expose the organs. Intestines and stomach were moved to the right side and hepatic lobes were delicately moved over the animal's thorax to allow access to the portal vein. A loose ligature carried out with surgical thread (Ethilon 5-0; Johnson & Johnson Intl., Brussels, Belgium) was then prepared around the portal vein downstream from the collateral vein near the hilum. Heparin (125 UI; Leo Pharmaceutical Products, Zaventem, Belgium) was injected in the inferior vena cava to avoid formation of intrahepatic microthrombi. One minute later, a 24-G catheter (Angiocath 0.7 × 19 mm; Becton-Dickinson, France) was inserted in the portal vein and the ligature was immediately tightened. At this moment, the perfusion flow was set to 14 mL/min to gently eject blood from the hepatic sinusoids. Special care was taken to avoid entry of air bubbles in the liver. The vena cava was immediately severed to avoid increase of blood pressure in the organ, and the liver was delicately excised and transferred into the perfusion tube. To compensate for the lack of hemoglobin in the perfusion solution, perfusion flow was brought to 28 mL/min once the preparation was finished. At this moment, the liver was introduced in a 25-mm o.d. tube. Livers were perfused for 1 hour, with the first 30 minutes in a recirculating mode followed by 30 minutes in a nonrecirculating mode as a rinsing step for elimination of the contrast agent from the perfusion circuit. All operative procedures related to animal care strictly conformed to the Guidelines of the French Government (licenses A 38 185 10 02 and 38 03 24) and fulfilled the requirements of the Committee of Ethics of our institutions.

Contrast Agent Protocol

Gd-EOB-DTPA (250 mM, ie, 39.25 g Gd/L, Primovist; Schering AG, Berlin, Germany) was used as hepatotropic contrast agent. The r_1 relaxivity values of Gd-EOB-DTPA at 0.47 T (20 MHz) are 8.7 $mM^{-1} \cdot s^{-1}$ in plasma and 16.6 $mM^{-1} \cdot s^{-1}$ in rat liver tissue at 37°C.[8]

The 250 mM Gd-EOB-DTPA solution was directly administered through the 120-mL perfusion medium as follows: 125 and 250 μL for MQCT experiments (final concentrations of 0.26 and 0.52 mM of perfusion medium) and 250 μL for MRI experiments (final concentration of 0.52 mM of perfusion medium).

Monochromatic Quantitative Computed Tomography Setup

A detailed description of the synchrotron instrumentation at the Biomedical Beamline of the ESRF (European Synchrotron Radiation Facility, Grenoble, France) was published in 1999.[19] Briefly, an electron beam is produced by a linear accelerator followed by a synchrotron booster and injected in a storage ring operated at 6 GeV and 200 mA.

A 21-pole wiggler (high magnetic field insertion device) with a maximum magnetic field of 1.4 T is used to enhance the x-ray beam intensity and the spectral range. The x-ray flux delivered by the ESRF ring exceeds the flux from a tungsten-anode x-ray tube by 5 orders of magnitude. This high intensity, associated with the tunability of the source, allows monochromatic beams to be generated in a wide range of energy. For the present experiment, the monochromator used a single bent Laue silicon crystal. Two monochromatic beams of 200-eV bandwidth and separated by 200 eV were created by a lead splitter. These beams (one above and one below the K edge) were deflected upward at a mean angle of 4.51° at 50.239 keV (Gd K-edge value) according to Bragg's law. They crossed at the center of the sample, after which they diverged and were recorded simultaneously on the dual line of the detector. The fan-shaped x-ray beam was 0.8 mm high and 120 mm wide. The attenuation profiles were measured with a cryogenically cooled, high-purity germanium detector made with 2 rows of 432 pixels of 0.35-mm width each and working in integration mode (Eurisys Mesure, Lingolsheim, France). The 2 lines allowed simultaneous measuring x-ray transmission of the sample at both energies. The digitized electronics provide a very large dynamic range. Two translation motors (horizontal and vertical, respectively) were used to preposition the sample and for multislice imaging. The acquisition was performed during a 360° rotation of the sample around the axis perpendicular to the beam. The time necessary to acquire the data corresponding to one slice (ie, to record 1440 projections) was approximately 24 seconds. Each perfused liver was inserted in a vertical Plexiglas tube, fixed on the motor unit, and then positioned at the beam-crossing point. Tubes filled with Gd-EOB-DTPA water solutions were taped and used as a reference for quantitative measurement during each beam time period. In chronologic order, for each experimental run, the solutions contained, respectively, 1.26 mg/mL (8 mM), 0.31 mg/mL (2 mM), and 0.47 mg/mL (3 mM) of Gd.

MQCT experiments were performed with a dual-energy subtraction technique. This technique uses the sharp rise in the photoelectric component of the attenuation coefficient of Gd at the binding energy of the K electron (K-edge value = 50.239 keV, $\Delta\mu/\rho$ = 14.73 cm^2/g). Two images obtained with monochromatic x-ray beams are simultaneously acquired, just below and above the K-edge of the contrast agent. The attenuation coefficient of Gd drastically increases when the absorption edge at 50.239 KeV is crossed, whereas the attenuation coefficients of cortical bone and brain tissue are comparatively not affected. The logarithmically subtracted image is derived from 2 cross-sectional images calculated (after correction for the nonuniform intensity distribution) from the numerous projections measured at small angular intervals. This is done thanks to a filtered backprojection algorithm running under an IDL (Interactive Data Language; RSI, Paris, France) software called the SNARK89 filtered backprojection algorithm.[27] The intensity scale of the subtraction image is proportional to the absorption as a result of Gd-labeled contrast agent[16] as explained below:

$$\Delta[\ln(I/I_0)] = \ln(I_b/I_0) - \ln(I_a/I_0) = [(\mu/\rho)_a - (\mu/\rho)_b]\,\rho_{Gd}\Delta X_{Gd} = \Delta(\mu/\rho)\,\rho_{Gd}\Delta X_{Gd} \quad (1)$$

where I_0 is the beam intensity before the sample, I is the beam intensity after the sample (with I_b and I_a, respectively, below and above the K edge), (μ/ρ) is the mass absorption coefficient at a given energy (in cm^2/g) (with $(\mu/\rho)_b$ and $(\mu/\rho)_a$, respectively, below and above the K edge), ρ_{Gd} the density (in g/mL), and X_{Gd} the thickness (in cm) of traversed contrast agent.

The absolute concentration of Gd (g Gd/mL) is calculated by dividing the logarithmic difference in intensity value of $\Delta[\ln(I/I_0)]$ by the known step of the mass absorption coefficient at the K edge ($\Delta(\mu/\rho)$ = 14.73 cm^2/g) because the X_{Gd} disappears in the integration procedure of the filtered backprojection algorithm. Therefore, subtracted images are Gd concentration maps. Such a concept has already been applied with success in clinical intravenous coronarography.[28] On the other hand, preclinical tomography experiments using dedicated software allowed the measurement of the absolute tissular concentration of the contrast agent from regions of interest (ROI) selected in the images. Using Gd phantoms, the minimal concentration detectable with the K-edge approach was estimated to be approximately 81 μg/mL of Gd.

Magnetic Resonance Imaging

Images were acquired on a 4.7-Tesla Avance 200 system (Bruker, Karlsruhe, Germany) equipped with a vertical magnet. T_1-weighted spin-echo sequences were used (NS = 3, slice thickness = 2.5 mm, interslice thickness = 4.2 mm, field of view [FOV] = 5 cm, matrix 256 × 256, TR = 300 ms, TE = 12 ms, NA = 2, total imaging time = 2 minutes 36 seconds). The spatial resolution was 0.2 mm. Livers, introduced in a 25-mm o.d. tube, were positioned at the isocenter of the magnet in a birdcage radiofrequency resonator. A tube containing 2 mM Gd-EOB-DTPA in aqueous gel (4% agar gel) was used as a reference for quantitative measurement. Before the administration of Gd-EOB-DTPA, fine-tuning and shimming of the field were performed on the proton-free induction decay of the sample. These settings remained unchanged for the rest of the experiment.

Imaging Protocols

MQCT: After acquisition of the precontrast image, the 250 mM Primovist solution was administered through the 120 mL perfusion medium at 2 different doses: 0.26 mM (n = 3) and 0.52 mM (n = 5). Images were then collected every

minute during a 5-minute period and every 5 minutes during the subsequent 25-minute period. The rinsing period with open circuit began immediately after the acquisition of the last image in the recirculating mode and washout images were collected every 5 minutes during the remaining 30 minutes of the protocol.

MRI: MRI experiments were performed in the optimal case obtained in MQCT, ie, 0.52 mM of Gd-EOB-DTPA. Note that the protocols of severed and clamped gallbladder were carried out as a result of the findings with the spared gallbladder. After acquisition of the precontrast image, the Primovist solution was administered through the perfusion medium (n = 10 livers for control perfusion, n = 4 for perfusion with severed gallbladder, and n = 5 for clamped gallbladder). Eight images were collected in the recirculating mode (at 2, 5, 8, 11, 15, 20, 25, and 30 minutes). The open circuit rinsing period began after the acquisition of the last image in recirculating mode and 6 images were collected every 5 minutes during the 30-minute rinsing period. These times correspond to the mean of the data acquisition period and are those reported in the graphs.

T_1 and T_2 Measurements

The same imaging system was used to estimate T_1 and T_2 values of the liver tissue after Gd-EOB-DTPA administration (n = 4). T_1 was estimated at 4.7 T (200 MHz) using an inversion-recovery sequence. Sequence parameters were TR = 2500 and 1500 ms, respectively, for precontrast and final images, TE = 7.1 ms, FOV = 5 cm, slice thickness = 1.5 mm, and matrix 64 × 64. For the precontrast image, TI ranged between 12.5 and 1500 ms and for the final image from 12.5 to 500 ms. T_1 was obtained by fitting with the following equation:

$$S_t = S_0[1 - (1 - cos\alpha)e^{-\frac{TI}{T_1}}] \quad (2)$$

where S_t and S_0 are the signal intensities measured at a given inversion time (TI) and after 5 T_1, respectively, and α is the flip angle.

T_2 was estimated through a spin-echo sequence (TR = 1000 ms, TE = 6.7 ms, NE = 24, FOV = 5 cm, slice thickness = 1.5 mm, matrix 64 × 64) and the following formula:

$$S_t = S_0(e^{-\frac{TE}{T_2}}) \quad (3)$$

Inductively Coupled Plasma Measurements

At the end of the MRI experiments, excised and perfused livers with spared gallbladder (n = 8), with severed gallbladder (n = 4), and with clamped gallbladder (n = 1) were dehydrated at 60°C in an incubator for 24 hours. The samples were digested and mineralized in a 3:1 vol/vol mixture of nitric acid (65%; Merck, Darmstadt, Germany)/hydrogen peroxide (30% in water; Janssen Clinica, Beerse, Belgium) by microwave treatment (Milestone; Analis, Namur, Belgium). Gd content was then determined by inductively coupled plasma atomic emission spectrometry (ICP-AES) (Jobin Yvon JY70+, Longjumeau, France). The same procedure was followed for the determination of Gd-EOB-DTPA concentrations in the livers used for the relaxivity measurements (n = 4).

Data Analysis

For both imaging techniques, image analyses were performed using circular regions of interest (ROIs) of approximately 0.25 cm^2 drawn in the liver, in the reference as well as in the perfusion medium, and carried over along all images of a given liver.

In the case of MRI, the signal was expressed as follows:

$$RE = \frac{\frac{I_i}{I_{ref,i}} - \frac{I_0}{I_{ref,0}}}{\frac{I_0}{I_{ref,0}}} \cdot 100 \quad (4)$$

where RE is the relative enhancement expressed as a percentage, I_0 and $I_{ref,0}$ are, respectively, the image intensities measured in the liver and in the reference before CA administration, and I_i and $I_{ref,i}$ are, respectively, the signal intensities in the liver and in the reference after CA administration.

MQCT images directly reflect the Gd concentration expressed in mg Gd/mL, as explained in the MQCT section (see previously).

Statistics

Data are given as the mean ± standard error of mean (SEM). The comparison between groups was performed with the paired *t* test and was considered to be significant at $P \leq 0.05$ and highly significant at $P \leq 0.01$.

RESULTS

Reference Samples

For MQCT, the concentrations obtained for the reference tubes were checked to be close to nominal values for each beam time period and during the whole duration of the experiment (1.34 ± 0.03 instead of 1.26 mg/mL [8 mM]; 0.30 ± 0.01 instead of 0.31 mg/mL [2 mM]; 0.53 ± 0.01 instead of 0.47 mg/mL [3 mM]). The ICP measurement gave a concentration equal to 7.71 mM (1.21 mg/mL) of Gd for the most concentrated reference.

For MRI, the signal intensity of the 2 mM Gd reference taped outside the perfusion tube was stable from mice to

mice, and small individual variations were taken into account in the RE calculation (see "Data Analysis" section).

Monochromatic Quantitative Computed Tomography

As expected, livers were not visible in the absence of contrast agent (control period) but became distinguishable at concentrations of 0.26 (not shown) and 0.52 mM after 10 minutes of perfusion (Fig. 1). It clearly appears that liver intensity increases during the contrast agent accumulation, reaches a plateau, and slightly decreases during the rinsing period.

Figure 2 highlights the quantitative results obtained after image analysis. At the highest dose (0.52 mM), 2 groups of mice are distinguishable toward the accumulation kinetic curve of Gd-EOB-DTPA. Although expected, it is worth mentioning that the curve obtained at the lowest dose exhibits the smallest evolution.

At both doses, the kinetic curves of Gd-EOB-DTPA show the same characteristics and are divided into 2 distinct phases: an uptake phase followed by the clearance of the contrast agent. After a few minutes of an initial stationary phase in which contrast agent administration had no effect on images, a significant contrast uptake appeared characterized by a slope depending on the contrast agent concentration. Elimination of the CA started 35 minutes after the beginning of the experiment (5 minutes after the rinsing) as a plateau followed by the decrease of CA concentration in the liver. It has to be mentioned that because of the dead volume of the perfusion line and the flow defined by the peristaltic pump, evolution of the contrast appears shifted as compared with the times of administration and washout of the contrast agent.

MRI: Perfusion With Gallbladder Spared (Same Protocol as Monochromatic Quantitative Computed Tomography)

Contrary to the situation encountered in MQCT, livers are always visible in MRI even without contrast agent

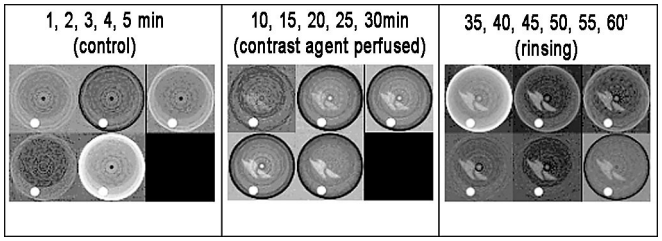

FIGURE 1. Monochromatic quantitative computed tomography kinetic study of a representative mouse liver perfused at a concentration of 0.52 mM. The white circular area is the 1.26 mg/mL (8 mM) Gd-EOB-DTPA reference solution. Circular artifacts observed in the pictures do not interfere with the signal evolution of the chosen region of interest.

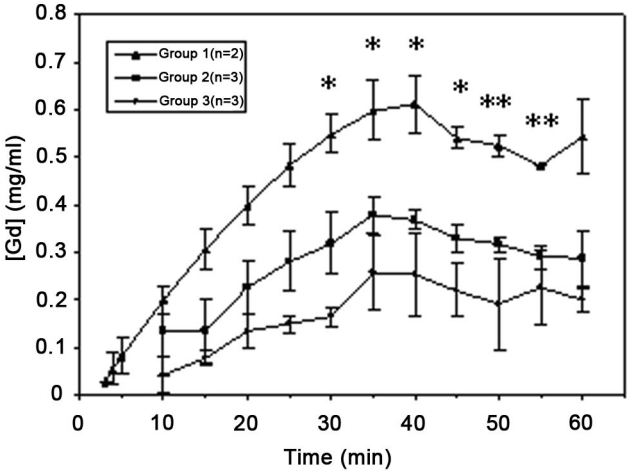

FIGURE 2. Curves representing the average of each group. The 2 groups of livers perfused with 0.52 mM of contrast agent are represented with ▲ (n = 2) and with ■ (n = 3), whereas livers perfused with 0.26 mM are represented with • (n = 3). *, statistically significant with regard to the other groups; **, highly significant with regard to the other groups.

(Fig. 3). The signal intensity of the liver (Fig. 4) increased drastically 5 minutes after contrast administration and started to decrease 10 minutes later. It continued decreasing for 10 minutes after the onset of the rinsing period and then increased again.

As seen in MQCT, 2 clear trends were also observed in MRI with regard to the accumulation and elimination of Gd-EOB-DTPA by the excised and perfused mouse liver in the case of spared gallbladder (in Fig. 4, respectively, group 1 = ▲ and group 2 = ■). The first group exhibited a larger contrast evolution than the second one, in which signal intensities decrease later and less rapidly. Although quantitatively different, these 2 behaviors have a similar signature characterized by 3 distinct phases. The first phase is a significant contrast uptake, apparently at the same rate for the 2 groups. The increase of signal intensity is caused by a T_1 effect resulting from the accumulation of the CA. Maximal signal intensity was slightly higher in the second group than in the first one. The subsequent phase takes place from the eighth to the 40th minute of perfusion. It is characterized by a decrease of intensity, slower in the second group than in the first one. This decrease of signal intensity is caused by the well-known T_2 effect resulting from a too high concentration of CA accumulated by the liver. Finally, the clearance of the contrast agent is characterized by a restoring of the signal intensity; this is the return to a T_1 effect resulting from the progressive elimination of Gd-EOB-DTPA.

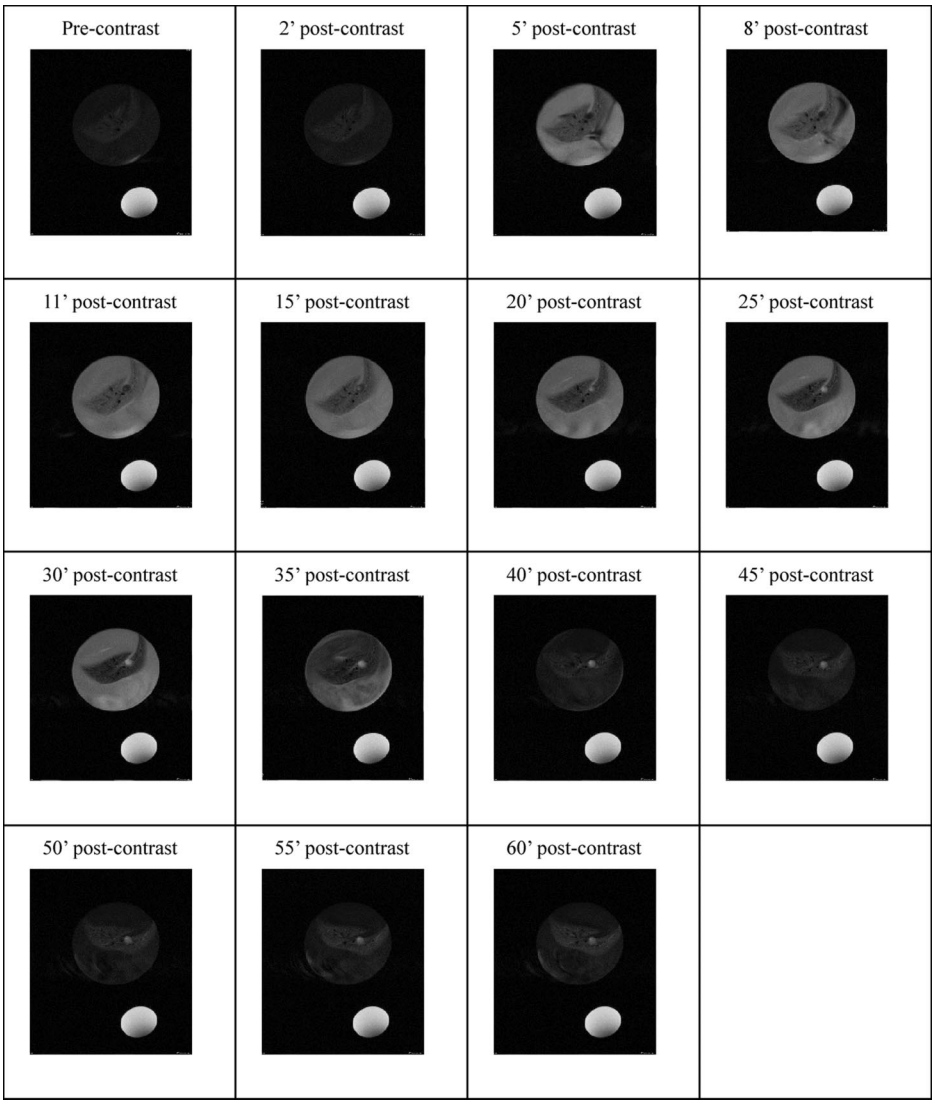

FIGURE 3. Magnetic resonance imaging kinetic study of a representative liver perfused with 0.52 mM Gd-EOB-DTPA. White circular area is the 2 mM Gd-EOB-DTPA reference solution.

As mentioned in the MQCT section, the evolution of the contrast is also shifted here with respect to the timing of the perfusion sequence.

MRI: Liver Perfusion With Gallbladder Severed and Clamped

Two complementary experiments were performed with MRI to understand the behaviors described here. In these experiments, the gallbladder was severed or clamped at the end of the surgery protocol.

Figure 4 shows the average kinetic curves of Gd-EOB-DTPA in all livers investigated by MRI, ie, livers of the 2 groups described previously and those with severed and clamped gallbladder. Livers with severed gallbladder follow the same behavior as livers of the first group, namely an earlier and more rapid decrease of signal intensity as compared with the second group.

By comparison, a lower increase of signal intensity shows that contrast agent accumulation is impaired in livers with clamped gallbladder. The final signal intensity in these livers returned to values close to those for the spared and severed gallbladder groups.

The characteristics of the clamped gallbladder group kinetic curve were different from those of the 3 other groups. After the same initial stationary phase, signal intensity increased to reach a maximum after 15 minutes of perfusion. After this maximum, the last phase was characterized by a slow and regular decrease of signal intensity until the end of the experiment.

Inductively Coupled Plasma

At the end of the MRI experiments, ICP measurements were performed to reflect the contrast agent concentration in the last image. It confirmed the presence of 2 distinct groups

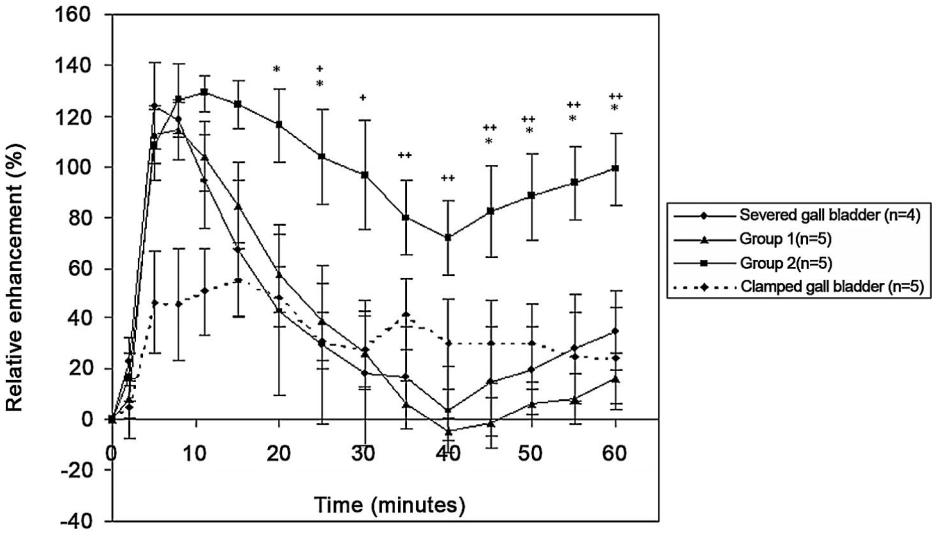

FIGURE 4. Relative enhancement expressed in percentage (RE %) as a function of time obtained on magnetic resonance images. The contrast agent concentration in the perfusion medium was 0.52 mM. As shown by monochromatic quantitative computed tomography, 2 behaviors appear in the case of perfusion with spared gallbladder. *, statistically significant regarding the others groups; +, statistically significant regarding group 2; ++, highly significant regarding group 2.

with respect to the amount of contrast agent accumulated by hepatic cells and confirmed that the first and severed gallbladder groups had the same behavior. Results were, in mM Gd, 4.51 ± 0.29, 9.88 ± 1.39, and 9.31 ± 1.69 and 0.15, respectively, for the second group, first group, livers with severed gallbladder, and those with clamped gallbladder (Fig. 5).

These results show that contrast agent concentration is twice as high in the first and severed gallbladder groups than in the second group, although MRI signal intensity remained higher in the latter than in the former. Livers with clamped gallbladder seemed to be unable to accumulate Gd-EOB-DTPA.

T_1 and T_2 Measurements in Liver Tissue at 4.7 T

T_2 decreases during the uptake of Gd-EOB-DTPA, confirming the loss of signal during the accumulation phase of the contrast agent. T_1 values are given in Table 1. The evolution of T_1 during perfusion cannot be determined because an image-per-inversion time must be acquired to extrapolate T_1. From T_1, T_2, and Gd concentration estimated by ICP in the final image, in situ relaxivities r_1 and r_2 were found to be 4.05 ± 0.23 and 9.43 ± 1.52 seconds^{-1}M^{-1}L, respectively.

TABLE 1. T_1 (in ms) in the Precontrast Image and in the Final Image of the Perfusion

	Precontrast	Final
Mouse 1	399	43
Mouse 2	275	61
Mouse 3	337	50
Mouse 4	361	43

Knowing the transverse and longitudinal relaxation times and the parameters of the image acquisition, intensity can be calculated according to the following equation:

$$I = e^{-\frac{TE}{T_2}}\left(1 - e^{-\frac{TR}{T_1}}\right) \quad (5)$$

Diamagnetic values were those measured in the precontrast image. Diamagnetic R_1 and R_2 were considered as constant throughout the perfusion.

Simulated curves shown that, despite the approximations and a lighter effect, 2 groups are distinguishable and several characteristics are encountered: strong increase of the contrast during the first minutes of the perfusion followed by a decrease and, finally, a restoring of the initial intensity during the rinsing period.

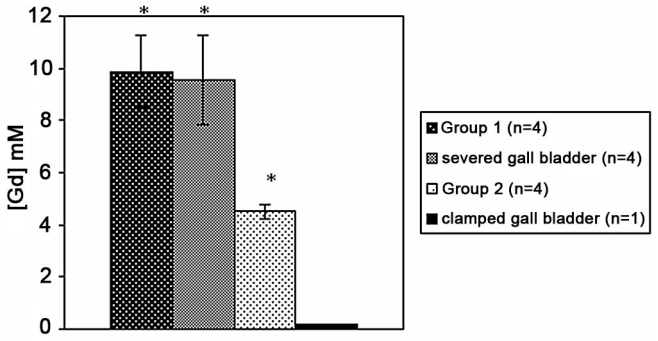

FIGURE 5. Final concentration of Gd-EOB-DTPA in livers as estimated by inductively coupled plasma. *, statistically significant regarding the others groups, except group 1 and the severed gallbladder group that are statistically identical.

DISCUSSION

The experiments performed show 2 main features: 1) the kinetic curves obtained in MQCT and MRI are different;

and 2) the behavior of livers toward the pharmacokinetics of Gd-EOB-DTPA can be separated into 2 distinct groups.

MQCT directly and unambiguously reflects the contrast agent concentration. As shown from the experimental data, the CA constantly accumulates in the liver during its delivery by the perfusion medium and is slowly eliminated during the rinsing period. Gd-EOB-DTPA concentrations in the liver were larger in organs perfused with the highest dose of contrast media. From the pharmacokinetic curves, 2 distinct behaviors clearly appear characterizing one group of livers (group 1) that accumulates more contrast agent than the other (group 2).

MRI and ICP quantitatively confirmed the MQCT data. However, in MRI, the signal intensity does not directly reflect the contrast agent concentration because of its multiparametric nature. After 10 minutes of perfusion, signal intensities began to decrease despite the continuing delivery of the contrast agent, a well-known paradoxic decrease resulting from the strong T_2 and T_2^* effects induced by a high concentration of the paramagnetic CA. As shown by ICP, the livers that had accumulated more contrast agent were livers in group 1, and those which had accumulated a smaller amount of contrast agent belong to group 2. Thus, MRI curves are inverted in comparison to MQCT curves.

Such groups do not exist in the case of rat liver perfusion.[22,23] To understand these 2 behaviors, perfusion of liver with severed and clamped gallbladder was performed. MRI and ICP revealed that the severed gallbladder behaved as the group taking up the highest concentration of Gd-EOB-DTPA and that the uptake was impaired in the case of clamped gallbladder. Impairment of contrast agent uptake in the clamped gallbladder arises from the fact that clamping significantly reduces the flux from liver to gallbladder, a process that induces inhibition of the uptake of Gd-EOB-DTPA by the anion organic transporter, which is a canal and thus energy-independent.

Although the reduced uptake in the group with clamped gallbladder is significantly larger than the one observed for the second group in the previous experiments, it can be suggested that the difference observed in the MQCT and MRI experiments between groups 1 and 2 results from a degradation (less drastic, however) of the physiological status of the liver during the experiments.

The existence of the 2 distinct groups probably comes from the perfusion protocol itself. The liver of a mouse is a small organ. When it is in the perfusion solution, flux generated by the peristaltic pump caused movements of the liver lobes. These motions could alter the circulation of the Krebs solution into the vasculature of the liver by clamping several vessels. At the same time, bile formation and excretion into the bile are altered by the same phenomenon.

Finally, there are some limitations of the perfusion model. These evaluations have been performed in healthy animals and not in tumor-bearing or diseased livers. Although Gd-EOB-DTPA has proved to be used for the evaluation of such pathologies, the model does not take account of the competition with endogenous bilirubin for hepatocyte uptake, which is not present in this perfusion model. Eventually, bilirubin is an important clinical factor that significantly alters the pharmacokinetic behavior of an anionic-mediated agent like EOB. Furthermore, the experiments have been performed on a perfused organ and not in an intact animal. They implied animal anesthesia we have performed by intraperitoneal injection of Nembutal, which belongs to the pentobarbital family. These compounds are known to alter cytochrome P-450 metabolism profiles in the liver and may alter the uptake and the clearance of Gd-EOB-DTPA. In fact, P-450 is the main cytochrome for drug detoxification. Gd-EOB-DTPA is not metabolized in the liver and so does not interact with cytochromes. We can conclude that anesthesia with Nembutal did not alter the pharmacokinetic of Gd-EOB-DTPA in our model of isolated and perfused mouse liver.

CONCLUSION

For the first time, MQCT and MRI have been performed to investigate the same pharmacokinetic problem. MRI is an ideal technique for diagnostics,[10,11] but the complex relationships between the contrast agent concentration and signal intensity makes it difficult to quantitatively follow pharmacokinetics. Contrarily, MQCT is a nearly real-time nondestructive and absolute procedure of quantification. ICP, a destructive analytic method, confirmed what was observed by MQCT. Kinetic curves in MQCT are easy to extrapolate, because it is possible to estimate the concentration of contrast agent, which is directly reflected by signal intensity. So the modality of accumulation of the contrast media can be followed in "real time." Finally, 2 groups of livers were identified in this protocol, but the physiological causes remain unclear. The existence of these 2 groups seems to arise from the instability of the perfusion protocol. Therefore, the isolated and perfused mouse liver model does not appear as a favorable system to be used in protocols for the study of the pharmacokinetics of a new contrast agent (or other drug) by the liver.

This pilot study has confirmed the validity of both approaches for the evaluation of the uptake of a hepatotropic contrast agent by the isolated and perfused mouse liver. Although less conveniently accessible, MQCT is the most direct approach to the quantitative measurement of the concentration of the contrast agent. This study has additionally demonstrated the peculiarity of the model of the isolated and perfused mouse liver which, contrary to the equivalent protocol carried out on rats, appears to be unstable, leading to an abnormal behavior characterized by an impaired uptake function.

ACKNOWLEDGMENTS

The financial support of the FNRS (Fonds National de la Recherche Scientifique) and of the French Community of Belgium (ARC Program 2000–2005) are acknowledged. The authors thank Mrs. Patricia De Francisco for her help in preparing the manuscript. The authors also thank the members of the ESRF Medical Beamline staff for their support during the MQCT experiments.

REFERENCES

1. Shuter B, Tofts PS, Wang SC, et al. The relaxivity of Gd-EOB-DTPA and Gd-DTPA in liver and kidney of the Wistar rat. *Magn Reson Imaging*. 1996;14:243–253.
2. Schmitt-Willich H, Brehm M, Ewers CL, et al. Synthesis and physicochemical characterization of a new gadolinium chelate: the liver-specific magnetic resonance imaging contrast agent Gd-EOB-DTPA. *Inorg Chem*. 1999;38:1134–1144.
3. Vander Elst L, Maton F, Laurent S, et al. A multinuclear MR study of Gd-EOB-DTPA: comprehensive preclinical characterization of an organ specific MRI contrast agent. *Magn Reson Med*. 1997;38:604–614.
4. Schuhmann-Giampieri G. Liver contrast media for magnetic resonance imaging. Interrelations between pharmacokinetics and imaging. *Invest Radiol*. 1993;28:753–761.
5. Clément O, Siauve N, Lewin M, et al. Contrast agent in magnetic resonance imaging of the liver: present and future. *Biomed Pharmacother*. 1998;52:51–58.
6. Planchamp C, Gex-Fabry M, Dornier C, et al. Gd-BOPTA transport into rat hepatocytes: pharmacokinetic analysis of dynamic magnetic resonance images using a hollow-fiber bioreactor. *Invest Radiol*. 2004;39:506–515.
7. Clément O, Mülher A, Vexler V, et al. Gadolinium-ethoxybenzyl-DTPA, a new liver-specific magnetic resonance contrast agent. Kinetic and enhancement patterns in normal and cholestatic rats. *Invest Radiol*. 1992;27:612–619.
8. Schuhmann-Giampieri G, Schmitt-Willich H, Wolf-Rudiger P, et al. Preclinical evaluation of Gd-EOB-DTPA as a contrast agent in MR imaging of the hepatobiliary system. *Radiology*. 1992;183:59–64.
9. Kuwatsuru R, Brash RC, Mülher A, et al. Definition of liver tumors in the presence of diffuse liver disease: comparison of findings at MR imaging with positive and negative contrast agents. *Radiology*. 1997;202:131–138.
10. Fujita M, Yamamoto M, Fritz-Zieroth B, et al. Contrast enhancement with Gd-EOB-DTPA in MR imaging of hepatocellular carcinoma in mice: a comparison with superparamagnetic iron oxide. *J Magn Reson Imaging*. 1996;6:472–477.
11. Marchal G, Zhang X, Ni Y, et al. Comparison between Gd-DTPA, Gd-EOB-DTPA, and Mn-DPDP in induced HCC in rats: a correlation study of MR imaging, microangiography and histology. *Magn Reson Imaging*. 1993;11:665–674.
12. Tonsok K, Takamichi M, Yasunori H, et al. Experimental hepatic dysfunction: evaluation by MRI with Gd-EOB-DTPA. *J Magn Reson Imaging*. 1997;7:683–688.
13. Weinmann HJ, Ebert W, Misselwitz B, et al. Tissue specific contrast agents. *Eur Radiol*. 2003;46:33–44.
14. Tsuda N, Kato N, Murayama C, et al. Potential for difference diagnosis with gadolinium–ethoxybenzyl–diethylenetriamine pentaacetic acid-enhanced magnetic resonance imaging in experimental hepatic tumors. *Invest Radiol*. 2004;39:80–88.
15. Dilmanian F, Garret RF, Thomlinson WC, et al. Computed tomography with monochromatic x-rays from the National Synchrotron Light Source. *Nuclear Instruments and Methods in Physics Research B*. 1991;56–57:1208–1213.
16. Dilmanian F, Wu XY, Parsons EC, et al. Single- and dual-energy CT with monochromatic synchrotron x-rays. *Phys Med Biol*. 1997;42:371–387.
17. Le Duc G, Corde S, Elleaume H, et al. Feasibility of synchrotron radiation computed tomography on rats bearing glioma after iodine or gadolinium injection. *Eur Radiol*. 2000;10:1487–1492.
18. Esteve F, Elleaume H, Bertrand B, et al. Coronary angiography with synchrotron x-ray source on pigs after iodine or gadolinium intravenous injection. *Acad Radiol*. 2002;9:92–97.
19. Elleaume H, Charvet AM, Berkvens P, et al. Instrumentation of the ESRF medical imaging facility. *Nuclear Instruments and Methods in Physics Research A*. 1999;428:513–527.
20. Le Duc G, Corde S, Charvet AM, et al. In vivo measurement of gadolinium concentration in a rat glioma model by monochromatic quantitative computed tomography: comparison between gadopentetate dimeglumine and gadobutrol. *Invest Radiol.* 2004;39:385–393.
21. Elleaume H, Charvet AM, Corde S, et al. Performance of computed tomography for contrast agent concentration measurements with monochromatic x-ray beams: comparison of K-edge versus temporal subtraction. *Phys Med Biol*. 2002;47:3369–3385.
22. Colet JM. Study of the mechanisms of hepatic internalisation of molecular and nanoparticular systems, potential contrast agents for magnetic resonance imaging [PhD thesis]. Mons, Belgium: University of Mons-Hainaut; 1995.
23. Colet JM, Van Haverbeke Y, Muller RN. Evidence for attachment of magnetic starch microspheres to Kupffer cells receptors in excised and perfused rat liver. *Invest Radiol*. 1994;29:223–225.
24. Colet JM, Pierart C, Seghi F, et al. Intravascular and intracellular hepatic relaxivities of superparamagnetic particles: an isolated and perfused organ pharmacokinetics study. *J Magn Reson*. 1998;134:199–205.
25. Colet JM, Lecomte S, Vander Elst L, et al. Cesium-133: a potential reporter of the hepatic uptake of contrast agents. *Magn Reson Med*. 2001;45:711–715.
26. Colet JM, Cetiner E, Hedlund BE, et al. Assessment of microvascular integrity in the isolated perfused rat liver by contrast-enhanced MRI. Attenuation of reperfusion injury by conjugated deferoxamine. *Magn Reson Med*. 1996;36:753–757.
27. Herman G, Lewitt RM, Ohdner D, et al. *SNARK89—A Programming System for Image Reconstruction from Projections*. Philadelphia: Medical Image Processing Group, Department of Radiology, University of Pennsylvania; 1989.
28. Elleaume H, Esteve F, Bertrand B, et al. First human transvenous coronary angiography at the European Synchrotron Radiation Facility. *Phys Med Biol*. 2000;45:39–43.